

Abundances and physical parameters for stars in the open clusters NGC 5822 and IC 4756. ^{*}

G. Pace¹, J. Danziger^{2,3}, G. Carraro⁴, J. Melendez¹, P. François⁵, F. Matteucci^{2,3}, and N. C. Santos¹

¹ Centro de Astrofísica, Universidade do Porto, Rua das Estrelas, 4150-762 Porto, Portugal

² INAF, Osservatorio Astronomico di Trieste, via G.B. Tiepolo 11, 34131 Trieste, Italy

³ Department of Astronomy, University of Trieste, via G.B. Tiepolo 11, 34131 Trieste, Italy

⁴ European Southern Observatory, Casilla 19001, Santiago, Chile

⁵ Observatoire de Paris, 64 Avenue de l'Observatoire, 75014 Paris, France

Preprint online version: February 16, 2019

ABSTRACT

Context. It has been suggested that the classical chemical analysis may be affected by systematics errors that would introduce abundance differences between dwarfs and giants. For some elements, the abundance difference could be real.

Aims. We address the issue by observing 2 solar-type dwarfs in NGC 5822 and 3 in IC 4756, and comparing their composition with that of 3 giants in either of the aforementioned clusters. We determine iron abundance and stellar parameters for dwarf stars. Then, abundances of calcium, sodium, nickel, titanium, aluminum, chromium, and silicon were determined for both giants and dwarfs. For the dwarfs, we also estimated the rotation velocities, and oxygen and lithium abundances. We improved cluster parameter estimates (distance, age, and reddening) by comparing existing photometry with new isochrones.

Methods. UVES high-resolution, high S/N ratio spectra were used. The width of cross correlation profiles was used to measure rotation velocities. For abundance determinations, the standard equivalent width analysis was performed differentially with respect to the Sun. For lithium and oxygen, we derived abundances by comparing synthetic spectra with observed line features.

Results. We find an iron abundance for dwarf stars equal to solar to within the margins of error for IC 4756, and slightly above for NGC 5822 ($[\text{Fe}/\text{H}] = 0.01$ and 0.05 dex respectively). The 3 stars in NGC 4756 have lithium abundances between $\text{Log } N(\text{Li}) \approx 2.6$ and 2.8 dex, the two stars in NGC 5822 have $\text{Log } N(\text{Li}) \approx 2.8$ and 2.5 respectively.

Conclusions. We show that, for sodium, silicon, and titanium, abundances of giants are significantly higher than those of the dwarfs of the same cluster (about 0.15, 0.15, and 0.35 dex). Other elements may also undergo some enhanced, but all within 0.1 dex. Indications of much stronger enhancements can be found using literature data. But artifacts of the analysis can be partly responsible for this.

Key words. Open clusters: individual: – stars: abundances

1. Introduction

Several efforts aimed at determining open cluster chemical abundances and parameters are being carried out, such as that of BOCCE (Bragaglia & Tosi 2006), in which chemical abundances of stars in the red clump of open clusters are measured (red clump stars are giants which are burning helium in their core). BOCCE, along with many other singular or coordinated efforts in which stars of different spectral type and luminosity

class are observed, greatly increased the database that could be employed to determine the Galactic abundance gradient (e.g. Carraro et al. 2007; Magrini et al. 2009; D’Orazi & Randich 2009; Paulson et al. 2003). These efforts are mainly aimed at studying the evolution with time of several phenomena occurring in stars, such as the depletion of light elements and chromospheric activity, as well as other features of the Galactic disk as a whole, such as the metallicity gradient and the age-metallicity relationship (e.g. Carraro et al. 1998; Friel et al. 2002; Magrini et al. 2009).

The choice of open clusters as preferred targets is justified by several advantages, viz. they are single stellar populations, i.e. ensembles of stars sharing common age, chemical composition and distance, they are distributed across the whole Galactic disk, and they span a wide range of ages. Only very young clusters tend to crowd close to spiral arms,

Send offprint requests to: G. Pace, e-mail: gpace@astro.up.pt

^{*} Based on observations collected at the European Organisation for Astronomical Research in the Southern Hemisphere, Chile, during the observing runs 073.D-0655 and 079.C-0131. Table 2 is only available in electronic form at the CDS via anonymous ftp to cdsarc.u-strasbg.fr (130.79.128.5) or via <http://cdsweb.u-strasbg.fr/cgi-bin/qcat?J/A+A/>

where they have recently formed (Dias & Lépine 2005). High resolution spectra allow us to measure the abundance of light elements, and in particular lithium, whose characteristics make it a useful probe of the mixing mechanisms in stellar envelopes. Very interesting results were obtained, for instance, by Smiljanic et al. (2009), by studying lithium and beryllium in several IC 4651 members at different evolutionary stages. Both elements are fragile, but are destroyed at different temperatures, i.e. in different layers, therefore probing the stellar interior at different depths.

In addition to the aforementioned issues, an important question addressed in the present work, for which open cluster suit particularly well, is whether the chemical composition changes during some evolutionary transition in the stellar life time. Sodium and aluminum have been found by several authors to be overabundant in giants belonging to several open clusters, for instance IC 4756, NGC 6939 and NGC 714 (Jacobson et al. 2007), NGC 6475 (Villanova et al. 2009), Collinder 261 (Friel et al. 2003), Berkeley 17 (Friel et al. 2005), Saurer 1 and Berkeley 29 (Carraro et al. 2004). For some other clusters only sodium overabundances has been detected in giants: IC 4651 (Pasquini et al. 2004), NGC 7789 and M 67 (Tautvaišienė et al. 2000; Tautvaišienė et al. 2005; Randich et al. 2006), and NGC 1817 and NGC 2141 (Jacobson et al. 2009). In some of these studies a direct comparison between evolved and unevolved stars was possible, and sodium and aluminum abundances in evolved stars were found to be higher than in dwarfs. In other studies the overabundances were detected just as an abundance ratio $[\text{Na-Al/Fe}]$ greater than 0.1 dex in giants or clump stars. Randich et al. (2006) argue that sodium enhancement in M 67 is to be ascribed to non-LTE effects affecting sodium lines in giants more than dwarfs, as discussed in Mashonkina et al. (2000). The extreme sensitivity of sodium to non-LTE effects was also noticed by Sestito et al. (2007). Wrong g_f values can also play a major role for giant stars, since, unlike for dwarf stars, the differential analysis with respect to the Sun may not overcome this problem. But in some of the clusters mentioned above, the effect may be in part real, since the amount of enhancement found significantly varies from cluster to cluster, even when the same kind of analysis is performed. In this case, aluminum and sodium enhancements may be due to internal processes.

Whether real or an artifact of the analysis, abundance differences between evolved and unevolved stars have important implications, because they mean that spurious differences may be found between stellar samples, if care has not been taken in comparing only dwarfs with dwarfs or giants with giants.

In the present study we analyse 5 solar-type stars in the open clusters IC 4756 and NGC 5822, and we compare our results with those from giants of the same clusters. These clusters were studied, together with other open clusters, by Santos et al. (2009). In this paper, iron abundances were analysed. Here we determine the chemical abundances of several other elements.

The paper is organised in the following way: in Sect. 2 we describe the sample and the observations. In Sect. 3 we report chemical abundance measurements with special emphasis on oxygen and lithium. An estimate of the projected rotation velocity of the sample stars is given in Sect. 4. We discuss the difference between giants and dwarfs, using both

our chemical abundance measurements and previously published results, in Sect. 5. In Sect. 6 we evaluate the cluster parameters by fitting isochrones to the colour-magnitude diagrams. Finally, we summarize the content of the paper in Sect. 7.

2. Observations and sample

The data analysed consist of UVES spectra of 5 dwarf and 6 giants members of NGC 5822 and IC 4756.

The observations of the dwarf stars were planned to study the evolution of chromospheric activity in solar-type stars, and carried out in the ESO observing run 073.D-0655. The clusters, IC 4756 and NGC 5822, were chosen mainly because of their intermediate age (about 1 Gyr, NGC 5822 being slightly younger than IC 4756). Target stars were selected among their solar-type, single members. Photometric study used for their choice, as well as target names, are from Herzog et al. (1975) for IC 4756 and from Twarog et al. (1993) for NGC 5822. For the same clusters, UVES spectra of 6 giants were available to us. A detailed description of the giant spectra is available in Santos et al. (2009) and will not be repeated here.

From 2 to 7 spectra were taken for each dwarf of the initial sample using UVES on the VLT at a resolution of about $R=100\,000$ in the red arm, which covers the range from 4800 to 6800 Å. Radial velocity measurements were used to strengthen single-member selection. They were obtained by cross-correlating stellar spectra with that of the Sun, by using the IRAF command *fxcor*.

We have detected the following double stars in IC 4756: HER 40, HER 150, HER 183, HER 189, and HER 294. HER 150, HER 189, and HER 294 are double lined, the other binaries were detected because of a radial velocity variation larger than $1\text{ km}\cdot\text{sec}^{-1}$. We were left with only 3 single members for this cluster, namely HER 97, HER 165, and HER 240, each having 2 observations on two different nights, and radial velocity differences of, respectively, 0.06, 0.20 and $0.40\text{ km}\cdot\text{sec}^{-1}$, which are explainable by measurement errors. Their radial velocities are: -24.9 , -25.7 , $-24.9\text{ km}\cdot\text{sec}^{-1}$, which confirm their membership, according to the mean cluster radial velocity of $-25.2\text{ km}\cdot\text{sec}^{-1}$ (Jacobson et al. 2007; Mermilliod et al. 2008). The cluster suffers from variable extinction (Schmidt 1978), therefore the photometric information we used to select the targets (Herzog et al. 1975) could not prevent us from including in the original sample a large proportion of double stars.

After adding the spectra, the resulting S/N ratio per pixel for these stars was about 50 in the blue arm and 100 in the red arm. HER 97 spectra are slightly poorer than those of the other two stars, which probably explains the larger difference between the 2 radial velocity measurements.

In NGC 5822, we observed TATM 11014 7 times, and TATM 11003 4 times in a total of 6 different nights. Their radial velocities for the individual observations have a standard deviation of about $0.5\text{ km}\cdot\text{sec}^{-1}$ for both, which we attribute to the measurement errors. The S/N of the single spectra can be, in fact, as low as 20.

The radial velocity of TATM 11003 is $-29.1\text{ km}\cdot\text{sec}^{-1}$, that of TATM 11014 is $-27.9\text{ km}\cdot\text{sec}^{-1}$. The mean radial velocities of the 20 confirmed members of NGC 5822 studied by Mermilliod & Mayor (1990) have a distribution whose mean value is $-29.31\text{ km}\cdot\text{sec}^{-1}$, with a standard deviation

of about $0.8 \text{ km}\cdot\text{sec}^{-1}$, thus confirming the membership of our target stars.

After adding all the spectra of each star, we achieved a S/N of 50 for the blue arm of TATM 11014 and slightly more than 100 for the red arm for the same star, and about 60 and 30 for the red and blue arm of TATM 11003.

We have also used some of the spectra used in Pace & Pasquini (2004), including the solar spectrum from the UVES archive, in order to calibrate the rotation velocity (Sect. 4) and measure lithium abundances (Sect. 3.2).

3. Chemical abundances

In order to measure stellar parameters of dwarf stars, i.e. temperature, gravity and microturbulent velocity, and the abundances of iron, calcium, sodium, nickel, titanium, aluminium, chromium, and silicon, we employed the same procedure and error analysis used in Pace et al. (2008), to which we refer the reader for a detailed description which will not be repeated here. Suffice it to say that we performed a standard EW analysis, i.e. we measured EWs and inferred abundances for each individual line (in the case of iron in two ionization states) by means of OSMARCS LTE models (Edvardsson et al. 1993), differentially line by line with respect to the Sun, and that the adopted atmospheric parameters were chosen among a grid of guess values. The only difference between the present analysis of dwarf stars and that in Pace et al. (2008), is that the temperature estimates about which the grids of parameters were constructed, were obtained from the B-V colours published in Herzog et al. (1975) and Twarog et al. (1993) through the calibrations in Soderblom et al. (1993) and Casagrande et al. (2006). To deredden the colours, we used the $E(B-V)$ values computed in Sect. 6.

As for giant stars, stellar parameters and iron abundances were already determined in Santos et al. (2009) using either the line list from Sousa et al. (2008) and that of Hekker & Meléndez (2007, HM). While effective temperature and gravity measurements in the two sets match to within the margins of error, the iron abundances obtained using HM are between 1 and 2σ higher. In Table 1 we show a comparison of our abundance and parameter measurements with those in Santos et al. (2009). Our results, indicated with “R06”, are obtained with the same method and same line list as for dwarfs. “S08” and “HM” indicate the results obtained using the line list from Sousa et al. (2008) and that from Hekker & Meléndez (2007). Our measurements, obtained using the same method and line list as for dwarfs, match with the results obtained employing HM, and we used them to proceed, in the same way as for dwarfs, with the measurement of calcium, sodium, nickel, titanium, aluminium, chromium, silicon and oxygen abundances. In Santos et al. (2009), the preliminary results of the dwarf iron abundances presented here were compared to the giant abundances. We do not have new elements to add to that discussion, and we will not repeat it here.

The equivalent width measurements and the relative individual abundances are available at CDS in electronic form (Table 2). Some of them are made automatically with the program ARES Sousa et al. (2007). We verified for a couple of stars that automatic and interactive measurements match no worse than two different sets of measurements made with the interactive method. The parameters found are indicated in Table 3. In Columns 2 and 3

we indicate the photometry from Twarog et al. (1993) and Herzog et al. (1975). To deredden B-V, we used the colour excesses obtained in Sect. 6. In the Column 4 and 5 we indicate the temperature obtained from the B-V colour by means of the calibrations of Soderblom et al. (1993) and Casagrande et al. (2006), while in Column 6 we indicate those obtained in the spectroscopic analysis. The difference between photometric and spectroscopic temperature is extremely large in all dwarfs, spectroscopic temperature being in all cases higher, as was mostly the case in Pace et al. (2008). If we consider photometric temperatures resulting from the calibration in Soderblom et al. (1993), such differences range from about 150 K to 600 K. Expressed in terms of B-V colour, the mismatch amounts to about 0.13 mag for both stars in NGC 5822 and range from 0.05 to 0.17 mag for the stars in IC 4756. The uncertainty in the colour excess computed in Section 6 amounts to 0.05 and 0.10 mag for NGC 5822 and IC 4756, respectively. These, together with the uncertainties in the (B-V)-versus-temperature calibration are unlikely to be the main cause of the discrepancy between spectroscopic and photometric temperatures, since, for instance, the calibration in Casagrande et al. (2006) has a standard deviation of about 50 K. In the case of IC 4756 the differential reddening (Schmidt 1978) and the larger photometric errors may account for the mismatch. In fact the spread of the main sequence is of the order of 0.2 mag. We may envisage that in both clusters there is probably a colour offset in the adopted photometry, possibly due to an inaccurate transformation from the instrumental to the standard magnitude system. A zero point difference of that order of magnitude of 0.1 mag or more, necessary to explain the mismatch between photometric and spectroscopic temperature, is not rare for photographic photometry when compared to modern CCD studies. In this context we urge new CCD photometry for both clusters. Therefore in this study we rely on the spectroscopic determinations of temperature, which are definitely more trustworthy.

In order to corroborate the last statement, we show in Figure 1 a comparison between 3 iron lines in the spectra of the Sun and those of HER 165 and HER 240, predicted to have close to solar temperature on the basis of the photometric calibrations of, respectively, Soderblom et al. (1993) and Casagrande et al. (2006). Our spectroscopic analysis indicates, instead, a higher temperature. On the top panel the observed spectra are plotted, on the center we show synthetic models of the iron lines obtained by using, for HER 240 and HER 165, the parameters found in the spectroscopic analysis, in the bottom we show the same spectral synthesis but with photometric temperature instead of the adopted one. The synthetic profiles based on spectroscopic temperatures resemble much more closely the observed ones. In particular, we notice that, assuming a photometric temperature for HER 240, its spectrum is expected to match almost exactly that of the Sun, which is not the case. The region indicated was chosen in order to contain several Fe I lines in a narrow range.

The results of the chemical analysis are summarised in Table 4. Errors in the $[X/H]$ values are those computed considering the uncertainty in the parameters and in the EWs, while the σ columns indicate the standard deviation of the measurements from individual lines. When only 2 or 3 lines are present, the standard deviation is replaced by half of the difference between the largest and the smallest

Star	T_{eff}			$\log G$		
	S08	HM	R06	S08	HM	R06
IC 4756 No38	5225±26	5151±73	5226	3.16±0.22	3.16±0.17	3.09
IC 4756 No42	5240±26	5217±89	5231	3.14±0.22	3.21±0.17	3.18
IC 4756 No125	5207±26	5146±82	5257	3.06±0.26	3.11±0.18	3.13
NGC 5822 No102	5253±28	5170±42	5260	3.17±0.39	3.20±0.13	3.28
NGC 5822 No224	5214±28	5237±65	5277	3.14±0.20	3.37±0.12	3.29
NGC 5822 No438	5208±25	5148±62	5208	3.16±0.19	3.21±0.11	3.19

Star	ξ			$[Fe/H]$		
	S08	HM	R06	S08	HM	R06
IC 4756 No38	1.40±0.02	1.22±0.11	1.35	0.05±0.08	0.08±0.11	0.09
IC 4756 No42	1.39±0.02	1.15±0.13	1.26	0.01±0.08	0.10±0.11	0.12
IC 4756 No125	1.47±0.02	1.31±0.13	1.23	0.02±0.08	0.07±0.11	0.10
NGC 5822 No102	1.44±0.03	1.18±0.07	1.28	0.00±0.08	0.05±0.06	0.04
NGC 5822 No224	1.41±0.03	1.15±0.08	1.29	0.06±0.08	0.22±0.08	0.21
NGC 5822 No438	1.39±0.02	1.13±0.08	1.19	0.06±0.08	0.18±0.08	0.14

Table 1. Comparison of abundance and parameter measurements for giants.

Star	V	B-V	$T_{Soder.}$	$T_{Casag.}$	T_{spec}	$\log G$	ξ
	mag			[K]		$[\log(g \text{ cm sec}^2)]$	$[\text{km}\cdot\text{sec}^{-1}]$
IC 4756							
HER 97	13.38	0.85	5512	5418	6118	4.46	1.29
HER 165	13.50	0.81	5658	5562	6070	4.45	1.24
HER 240	13.48	0.76	5848	5753	6007	4.54	1.21
NGC 5822							
TATM 11003	14.662	0.769	5625	5546	6160	4.74	1.05
TATM 11014	14.448	0.732	5764	5685	6273	4.74	1.26

Table 3. Stellar parameters.

value. Iron abundances in giant stars and relative errors are from Santos et al. (2009).

3.1. Oxygen abundances

For oxygen abundances the only line available to us is the forbidden O I line at 6300.30 Å, which is very weak and often contaminated by telluric lines. We analysed it with MOOG (Snedden 1973, version 2002) and Kurucz models (Kurucz 1993). The line is blended with that of Ni I at 6300.336 Å. As in Randich et al. (2006) and Pace et al. (2008), we assumed a $\log gf$ value of -2.11 for the oxygen line and -9.717 for that of the nickel. In order to measure abundances in dwarfs, we selected the spectra for which the telluric lines did not overlap with the oxygen profile. Even after summing these spectra, the S/N ratio at the wavelength of interest remained too low to reliably measure the EW of the the blended feature or to compare the spectra with a synthetic model. We could only set an upper limit. Comparing the stellar feature with that of the UVES–archive solar spectrum, we noticed that, in all the cases, the solar feature was well suited as an upper limit for the stellar one. We employed the driver synthe of MOOG, giving as fixed input the stellar parameters and nickel abundances obtained as described above, to build the

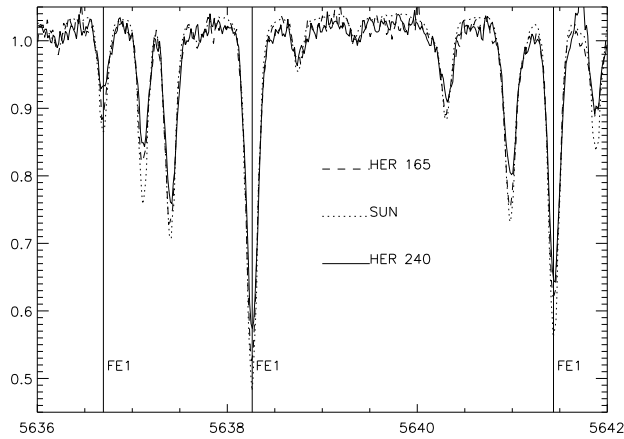
models of our stars; we then searched for the oxygen abundances for which the synthetic spectrum matched with the solar one, thus finding an upper limit for the stellar oxygen abundance. For the Sun itself, the match between synthetic and observed profile was achieved by assuming: $\text{Log}(\text{O}/\text{H})+12=8.83\pm0.03$. This value was subtracted from all the stellar values previously obtained, in order to find an upper limit for $[\text{O}/\text{H}]$. For all the 3 stars in IC 4756, we claim that $[\text{O}/\text{H}] \leq 0.15$ dex. According to the feature of HER 165, which is comparable to that of the Sun, we estimate that the oxygen abundance in this star is not much lower than the aforementioned upper limit, but, owing to the scantiness of the data on which it depends, this conclusion must be taken with caution. For NGC 5822 dwarfs, we could find only an upper limit of 0.3 dex.

Despite having at our disposal very good spectra for giants, we could not obtain precise measurements because the oxygen line was blended with the telluric feature at 6299 Å, and no calibration target was available to us. The center of the telluric line coincided exactly with that of the oxygen line in IC 4756 spectra, resulting in a single gaussian feature. In NGC 5822 spectra, the two line centers were distant enough to originate a slightly asymmetric feature, but in no case was it possible to have dependable results from the comparison of the observed spectra with the synthetic

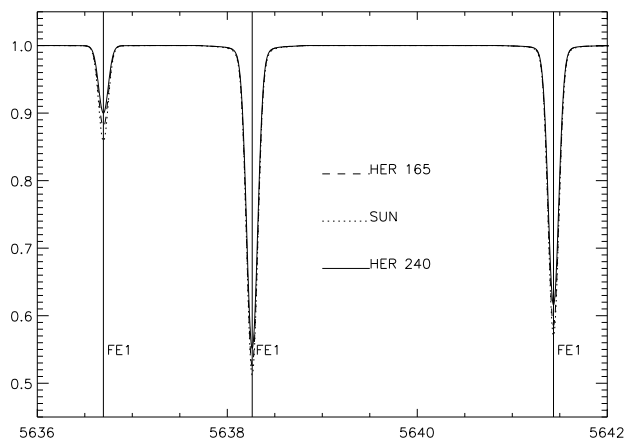
Star or Cluster name	Fe I			Na I			Al I			Si I		
	[X/H]	N	σ	[X/H]	N	σ	[X/H]	N	σ	[X/H]	N	σ
	dwarfs											
HER 165	0.05± 0.09	62	0.04	-0.10± 0.06	3	0.03	-0.01± 0.05	1	0.00	0.01± 0.02	8	0.04
HER 240	-0.02± 0.09	62	0.05	-0.17± 0.06	3	0.06	-0.20± 0.05	2	0.04	-0.06± 0.02	8	0.03
HER 97	0.00± 0.09	61	0.06	-0.18± 0.06	3	0.08	-0.06± 0.05	1	0.00	-0.07± 0.03	8	0.03
	mean dwarf											
IC 4756	0.01			-0.15			-0.09			-0.04		
	giants											
No 38	0.08± 0.11	16	0.08	0.19±0.04	3	0.04	-0.04±0.03	2	0.03	0.10±0.02	9	0.06
No 42	0.10± 0.11	15	0.08	0.23±0.03	3	0.05	-0.03±0.03	2	0.05	0.11±0.02	9	0.06
No 125	0.07± 0.11	15	0.08	0.16±0.04	3	0.04	-0.03±0.03	2	0.04	0.09±0.02	9	0.05
	mean giant											
IC 4756	0.08			0.19			-0.03			0.10		
	dwarfs											
TATM 11014	0.07± 0.09	49	0.05	-0.11± 0.06	3	0.05	-0.05± 0.05	1	0.00	0.04± 0.03	6	0.03
TATM 11003	0.02± 0.09	57	0.07	-0.19± 0.06	2	0.03	–	–	–	-0.01± 0.03	7	0.05
	mean dwarf											
NGC 5822	0.05			-0.15			-0.05			0.01		
	giants											
No 102	0.05± 0.06	13	0.04	0.15±0.03	3	0.09	-0.04±0.02	2	0.09	0.03±0.02	9	0.09
No 224	0.22± 0.08	14	0.06	0.26±0.03	3	0.05	0.05±0.02	2	0.06	0.18±0.02	9	0.07
No 438	0.18± 0.08	16	0.06	0.23±0.03	3	0.05	0.05±0.02	2	0.05	0.20±0.02	9	0.12
	mean giant											
NGC 5822	0.15			0.21			0.02			0.14		
	Ca I			Ti I			Cr I			Ni I		
	dwarfs											
HER 165	0.10± 0.08	9	0.04	0.02± 0.10	11	0.06	0.05± 0.11	6	0.05	-0.03± 0.06	21	0.05
HER 240	-0.01± 0.08	11	0.03	-0.05± 0.10	10	0.06	0.00± 0.11	6	0.05	-0.09± 0.06	22	0.05
HER 97	0.06± 0.08	11	0.06	-0.08± 0.10	11	0.12	-0.04± 0.11	5	0.04	-0.07± 0.07	20	0.07
	mean dwarf											
IC 4756	0.05			-0.04			0.00			-0.06		
	giants											
No 38	0.06±0.05	9	0.04	0.11±0.07	9	0.08	0.08±0.07	6	0.03	0.03±0.03	23	0.07
No 42	0.09±0.05	9	0.05	0.15±0.07	9	0.09	0.14±0.07	6	0.03	0.05±0.03	23	0.07
No 125	0.03±0.05	9	0.05	0.08±0.07	9	0.08	0.05±0.07	6	0.04	0.05±0.03	23	0.08
	mean giant											
IC 4756	0.06			0.11			0.08			0.04		
	dwarfs											
TATM 11014	0.09± 0.08	9	0.05	0.01± 0.09	6	0.07	0.11± 0.10	6	0.04	-0.01± 0.06	21	0.06
TATM 11003	0.06± 0.08	9	0.04	-0.02± 0.10	9	0.04	0.04± 0.11	6	0.10	-0.06± 0.06	19	0.07
	mean dwarf											
NGC 5822	0.08			0.00			0.07			-0.03		
	giants											
No 102	0.02±0.03	9	0.06	0.07±0.05	9	0.08	0.09±0.05	6	0.05	-0.11±0.02	23	0.09
No 224	0.16±0.03	9	0.07	0.28±0.05	9	0.08	0.24±0.05	6	0.03	0.17±0.02	23	0.10
No 438	0.14±0.03	9	0.05	0.19±0.05	9	0.09	0.21±0.05	6	0.03	0.14±0.02	23	0.09
	mean giant											
NGC 5822	0.11			0.18			0.18			0.07		

Table 4. Results of the chemical analysis.

Observed spectra



Synthesis using spectroscopic temperatures



Synthesis using photometric temperatures

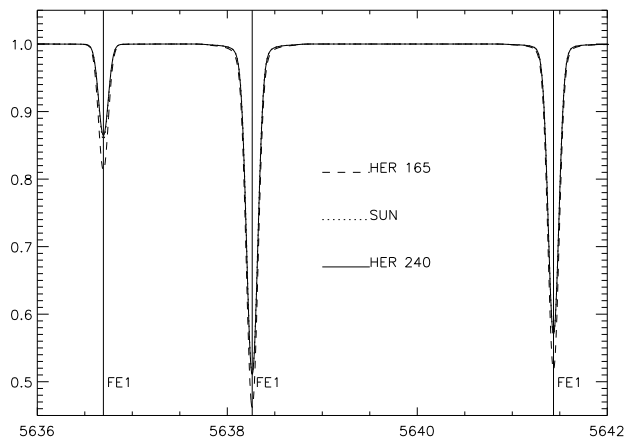


Fig. 1. Comparison of the spectra of HER 240 and HER 165 with that of the Sun.

ones. However, the telluric line at 6302 \AA was isolated, and its EW ranged from 15 to 25 m\AA in all the spectra. The telluric line at 6299 \AA , blended with the oxygen line, is a few percent stronger. Using this piece of information, we inferred that oxygen abundances in giants of both IC 4756

and NGC 5822 must be in the range of values from -0.1 to 0.15 dex. Unfortunately, the direct comparison of giants and dwarfs in the same cluster on the basis of these rough estimations, does not add relevant information.

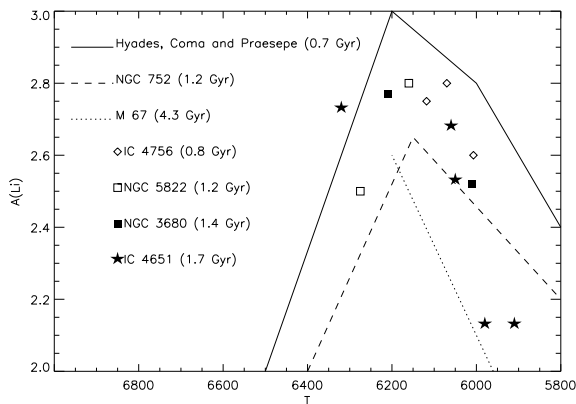
3.2. Lithium

Lithium abundances were obtained analysing the lithium doublet at 6707.8 \AA . Adopting a procedure similar to that used for oxygen, we employed the driver *synthe* of MOOG, the line list from Israelian et al. (2001), and Kurucz models obtained with the stellar parameters measured above, to produce synthetic spectra in the wavelength interval encompassing the lithium line profile, and searched for the lithium abundance for which the best match with the observed feature is achieved. We could obtain reliable measurements, as the profiles are quite strong in our stars. The typical errors, judged by the extension of the lithium abundance range for which the match was acceptable, are between 0.05 and 0.15 dex. If we adopt the conservative estimate of the error in the temperature of 110 K as in Pace et al. (2008), this will lead to an uncertainty in the lithium abundance of 0.1 dex, which will therefore lead to a typical maximum error of about 0.15 dex. The other parameters hardly affect the lithium abundance determination. Using the same procedure, we also compared the synthetic spectrum of the Sun with the UVES–archive solar spectrum, and we found that we obtained the best match by assuming $A(\text{Li})=1$ rather than the canonical $A(\text{Li})=1.1$ where $A(\text{Li})$ is, as customary, $\text{Log}(\text{Li}/\text{H})+12$.

Since we believe that a more precise temperature scale may further our understanding of lithium depletion (cfr. Sect. 3.2) and errors in the colour excess may introduce a cluster to cluster bias in the temperature determinations (cfr. Sect. 3), we also measured lithium abundances in those stars of the sample of Pace et al. (2008) for which data in the literature were based on photometric temperatures, and whose parent clusters are significantly reddened and whose photometric temperatures, as a consequence, were uncertain. The results of our lithium abundance measurements are shown in Table 3.2, in dex, along with temperature, in Kelvin, and gravity, in unit of $\log(g\text{-cm}\cdot\text{sec}^{-2})$. Typical uncertainties are of about ± 0.1 dex. Since, using the same method, the Sun is found to have $A(\text{Li})=1.0$, the data are probably best comparable with literature sources by adding a positive offset of 0.1 dex. Effective temperatures coming from the spectroscopic analysis in this paper and in Pace et al. (2008) are also shown.

In Figure 2 we also show a temperature versus lithium abundance diagram, in which we compare the 12 data points from the present analysis, shown in Table 3.2, with published open cluster data at 3 different ages. Hyades, Coma and Praesepe data are depicted in one single curve, another represents NGC 752 and the third M 67. M 67 data are taken from Pasquini et al. (2008), the remainder from the compilation in Xiong & Deng (2009). The curves that represent the published cluster data at the 3 different ages, are fits by eye to the datapoints. The ages indicated are taken from Salaris et al. (2004). The temperatures for the Hyades age clusters and NGC 752 are derived from photometry. For the former the uncertainty in the colour excess should not play a major role, since they are nearby clusters.

Star	A(Li)	T_{eff}	logG
Present sample			
IC 4756 ([Fe/H]=0.01 dex)			
HER 97	2.75	6118	4.46
HER 165	2.8	6070	4.45
HER 240	2.6	6007	4.54
NGC 5822 ([Fe/H]=0.05 dex)			
TATM 11003	2.8	6160	4.74
TATM 11014	2.5	6273	4.74
Sample of Pace et al. (2008)			
IC 4651 ([Fe/H]=0.12 dex)			
AHTC 1109	2.7	6060	4.55
AHTC 2207	2.5	6050	4.36
AHTC 4220	2.1	5910	4.57
AHTC 4226	2.1	5980	4.44
Eggen 45	2.7	6320	4.43
NGC 3680 ([Fe/H]=-0.04 dex)			
Eggen 70	2.8	6210	4.47
AMC 1009	2.5	6010	4.50

Table 5. Lithium abundance measurements.

Fig. 2. Comparison of lithium abundances in different open clusters.

The additional 12 points introduced in Figure 2 clearly do not resolve the problem of lithium in Solar type stars. Nevertheless the steeper decline of lithium abundance in IC 4651 suggests that a study of a larger sample of stars in this cluster would be warranted.

4. Rotation velocity

In Pace & Pasquini (2004) using available UVES spectra, we obtained the cross-correlation profile with a suitable template (courtesy of C. Melo) and measured its FWHM for a set of stars with published $v \cdot \sin i$ taken with the same

Star	FWHM [pixels]	$v \sin i$ [km-sec ⁻¹]	dev. [km-sec ⁻¹]
Sun	5.46	2.0	-2.0
stars in IC 4651:			
AT 1228	17.74	15.7	-1.9
Eggen 15	11.76	10.0	-1.6
Eggen 34	32.19	25.2	0.9
Eggen 45	7.56	4.2	-0.3
Eggen 79	25.6	21.8	-1.3
Eggen 99	36.28	28.1	1.4
star in NGC 3680:			
Eggen 60	7.10	1.9	1.3

Table 6. Data used to calibrate the $v \sin i$.

configuration as for those of the targets; we had found the values of A and B that minimise the χ^2 in the relationship:

$$v \cdot \sin i = A \cdot \sqrt{FWHM^2 - B^2}$$

We then used that relationship with the computed values of A and B , to measure target-star $v \cdot \sin i$ from the FWHM of their cross-correlation profile. We repeated in the present paper the calibration with the same stars. This time, cross-correlation profiles of calibration and target stars were obtained with the IRAF command *fxcor* using the upper red arm of UVES spectra (from 5800 to 6800 Å) and, as a template, the UVES archive solar spectrum. This new calibration made our measurements easier to reproduce. Calibration data – namely star names, FWHM and $v \sin i$ measurements, and deviations from the fit – are shown in Table 6. We found the following values for the parameters in the equation above: $A = 0.82$ [km-sec⁻¹], $B = 5.93$ pixels, giving a root mean square of the data points around the fit of 1.5 km-sec⁻¹. We adopt this value as an estimate of the uncertainty in the $v \sin i$ measurement due to the calibration: Δ_{cal}

The results on projected rotation velocities are given in Table 7. We also computed the error in FWHM from the standard deviation of the FWHM measurements performed on the individual spectra, and when only two spectra were available for a given star, half of the difference between the two measurements were used. The error in FWHM measurement was found to be much less important than Δ_{cal} . However, the results must be taken only as a rough estimate. The stars of our sample appear to rotate slightly faster than the Sun, for which $v \sin i = 2$ km-sec⁻¹, and roughly similar to the solar stars in IC 4651 and NGC 3680. The presence of such slow rotators in young clusters is not surprising, since Pace & Pasquini (2004) measured low values of $v \sin i$ also in Hyades and Praesepe stars. The data presented in Table 7 alone, is not sufficient to allow us to draw conclusions about the evolution of angular momentum in solar type stars.

5. Comparison of our chemical abundances with previous results.

In Table 8 we compiled abundance measurements available in the literature, made by means of spectroscopic studies.

Cluster	source	[Fe/H]	[Na/H]	[Al/H]	[Si/H]	Ref
IC 4756	3 dwarfs	0.01 $\sigma=0.04$	-0.15 $\sigma= 0.04$	-0.09 $\sigma=0.05$	-0.04 $\sigma=0.04$	1
IC 4756	1 dwarf	0.03 –				4
IC 4756	3 giants	0.08 $\sigma=0.02$	0.19 $\sigma= 0.04$	-0.03 $\sigma=0.05$	0.10 $\sigma=0.01$	1,2
IC 4756	7 giants	0.0 ± 0.1 *				3
IC 4756	4 giants	-0.05 ± 0.04				4
IC 4756	1 giant			0.20	0.16 ± 0.25	4
IC 4756	6 giants	-0.15 $\sigma=0.04$	0.73 $\sigma= 0.06$ *	0.44 $\sigma=0.08$ *	0.19 $\sigma=0.06$	5
NGC 5822	2 dwarfs	0.05 $\sigma=0.03$	-0.15 $\sigma= 0.04$	-0.05 –	0.01 $\sigma=0.02$	1
NGC 5822	3 giants	0.15 $\sigma=0.08$	0.21 $\sigma= 0.04$	0.02 $\sigma=0.01$	0.14 $\sigma=0.08$	1,2
NGC 5822	3 giants	0.12 $\sigma=0.1$				4
NGC 5822	1 giant		0.28 ± 0.07	0.12 ± 0.12	0.25 ± 0.25	4
		[Ca/H]	[Ti/H]	[Cr/H]	[Ni/H]	
IC 4756	3 dwarfs	0.05 $\sigma=0.05$	-0.04 $\sigma= 0.05$	0.00 $\sigma=0.05$	-0.06 $\sigma=0.03$	1
IC 4756	3 giants	0.06 $\sigma=0.03$	0.11 $\sigma= 0.03$	0.08 $\sigma=0.03$	0.04 $\sigma=0.01$	1,2
IC 4756	1 giant	-0.06 ± 0.29	-0.28 ± 0.29		0.04 ± 0.16	4
IC 4756	6 giants	-0.08 $\sigma=0.08$			-0.07 $\sigma=0.05$	5
NGC 5822	2 dwarfs	0.08 $\sigma=0.02$	0.00 $\sigma= 0.02$	0.07 $\sigma=0.04$	-0.03 $\sigma=0.03$	1
NGC 5822	3 giants	0.11 $\sigma=0.07$	0.18 $\sigma= 0.11$	0.18 $\sigma=0.08$	0.07 $\sigma=0.14$	1,2
NGC 5822	1 giant	-0.05 ± 0.23	0.20 ± 0.24	0.26 ± 0.29	0.25 ± 0.26	4

Table 8. Compilation of abundance determinations in the literature from spectroscopic data. References: (1) Present work; (2) Santos et al. (2009); (3) Gilroy (1989); (4) Luck (1994); (5) Jacobson et al. (2007)

Star	FWHM [pixels]	$v \sin i$ [km·sec ⁻¹]
IC 4756		
HER 165	6.9	3
HER 97	8.1	5
HER 240	7.0	3
NGC 5822		
TATM 11014	8.9	5
TATM 11003	7.1	3

Table 7. $v \sin i$ estimations of our target stars.

We indicated the dispersion of the measurements, using either their standard deviation or, when only 3 or 2 measurements were available, half of the difference between the highest and lowest value. The measurements given by Gilroy (1989) (flagged with an asterisk) have only one significant digit, and for 5 out of 7 stars resulted to have $[\text{Fe}/\text{H}]=0.0$ dex. The value indicated in this table is more representative of her results than the mean of the 7 measurements (which would be 0.04 dex). The measurements by Jacobson et al. (2007) marked with an asterisk refer to the EW analysis result. Spectral synthesis would indicate an enhancement 0.06 dex higher for sodium and 0.11 dex lower for aluminum.

We notice that iron abundance measurement of giants in IC 4756 made by Jacobson et al. (2007) are substantially lower than any other quoted result, including that of the present analysis and of Santos et al. (2009). Jacobson et al. employed Hydra/WIYN spectra at a resolution of $R \approx 15\,000$, whose S/N range from 75 to 150 per pixel, and whose spectral coverage is 300 Å, enough to include more than 20 Fe I lines and 3 or 4 Fe II lines. Furthermore, they analysed 6 giants, and the measurements show little spread. Sousa et al. (2007) showed that, for a spectrum of a dwarf with signal to noise of about 100 per pixel, at resolutions lower than $R \approx 30\,000$, EWs are systematically underestimated. For $R=15\,000$, this effect is of about 10%, leading to abundance errors that might explain the mismatch between our results and those of Jacobson. Giants are likely to suffer from this effect even more, due to their higher line crowding. However, when it comes to abundance ratios $[\text{X}/\text{Fe}]$, these effects, which affect both sides of the ratio, should compensate each other.

Data shown in Table 8, indicate that there is a difference in the chemical composition between giants and dwarfs. In particular, sodium abundance is significantly enhanced in giants. The huge discrepancy between different amount of enhancements found, e.g. between the present work and Jacobson et al. (2007), is mainly due to the use of a different line list. In fact, they claim that, using the same line list we employed (Randich et al. 2006), they would find $[\text{Na}/\text{H}]=0.2$, which matches our result for giants.

6. Revision of clusters' fundamental parameters.

The new iron abundance estimates we provide in this paper offer us the possibility of revising the cluster fundamental parameters - namely distance, reddening and age - on a more solid basis. Therefore, we assembled available photometry from the literature, and created Colour Magnitude Diagrams (CMD). We adopted Herzog et al. (1975) photographic photometry for IC 4756 and Twarog et al. (1993) CCD photometry for NGC 5822. The two CMDs are shown in the right and left panel of Fig. 3, respectively. We transformed iron abundances values from the logarithmic scale relative to the Sun ($[\text{Fe}/\text{H}]$) into the linear scale (Z) using the relation $[\text{Fe}/\text{H}] = \log(Z/0.019)$ from Carraro et al. (1999). We then generated isochrones for that value of Z . We obtained $Z = 0.019$ for IC 4756 and $Z = 0.021$ for NGC 5822. In Fig. 3 we show the best *by eye* fit we achieved after several trials. The fit to the CMD of NGC 5822 (left panel) is good. It provides the following set of parameters: $E(B-V) = 0.1 \pm 0.05$, $(m-M) = 9.9 \pm 0.1$, and age = 1.0 ± 0.1 Gyr. This, in turn, yields a heliocentric distance of 830 pc. The CMD of IC 4756 has a much larger spread and a secondary Main Sequence (MS), presumably produced by binary stars, and which seems to be as populated as the single star MS. For this cluster our parameters are: $E(B-V) = 0.15 \pm 0.10$, $(m-M) = 8.6 \pm 0.1$, and age = 0.8 ± 0.2 Gyr. This, in turn, yields a heliocentric distance of 430 pc.

As noted in Section 3, the huge differences between photometric and spectroscopic temperatures, point to a zero point error in the photometry, of roughly 0.13 mag for NGC 5822, and of the same order of magnitude for IC 4756 but more difficult to evaluate due to the differential reddening. This can explain the difference between the extinctions obtained in this Section and those obtained in the extinction maps of Hakkila et al. (1997) as described in Meléndez et al. (2006). The aforementioned zero-point error affects the present evaluation of the cluster parameters of an amount that has to be added to random errors (the errors given above include it). The age, evaluation, however, are not significantly affected by this.

In both cases we stress the need for improved photometry to reach fainter magnitudes along the MS, and comparison fields to deal with contamination. This is of primary importance for at least two reasons. Firstly, more precise age estimates will allow us to confirm or revise the conclusions reached in Pace et al. (2009) concerning the evolution of chromospheric activity. Secondly, we will be able to say whether the cause of the discrepancy between photometric and spectroscopic temperatures resides completely in the photometry, as we suspect, or a systematic error in our spectroscopic temperature determinations is present and should be corrected for.

7. Conclusions.

We have analysed high resolution spectra of 5 solar-type stars in IC 4756 and NGC 5822, in order to obtain their parameters, chemical composition, including lithium abundances, and rough estimates of their projected rotation velocities. While iron abundances, in most of the cases, give results, consistent within the errors, with those of previous studies based on giants of the same clusters, sodium, aluminum and silicon, present very high enhancements in giants in IC 4756. This finding matches with published

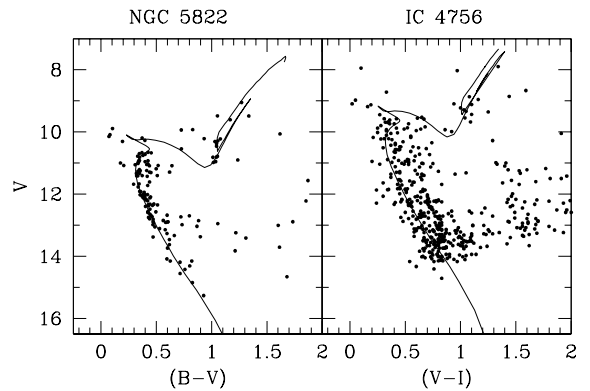


Fig. 3. CMD and fit of isochrones for NGC 5822 and IC 4756.

results regarding several other open clusters (see Section 1). Whether these abundance enhancements are real or due to systematic errors, they have important implications (De Silva et al. 2009); for example on the studies on the Galactic bulge: when comparing the bulge with the disk, the same type of stars in both populations should be used. In the first studies of this kind employing high-resolution spectroscopy, this was not yet possible for a sufficient number of targets (Fulbright et al. 2007; Lecureur et al. 2007; Zoccali et al. 2006). But works are presently available that compare bulge giants with disk giants (e.g. Meléndez et al. 2008; Alves-Brito et al. 2010; Ryde et al. 2010) or bulge dwarfs with disk dwarfs, taking advantage of the microlensing effect (e.g. Bensby et al. 2009).

The rotation velocity of our sample stars is slightly larger than that of the Sun, roughly between 3 and 5 $\text{km}\cdot\text{sec}^{-1}$, a smaller range than observed in other clusters of comparable age.

Cluster parameters are computed using published photometry and the iron abundance obtained in the spectroscopic analysis. We found an age of 1 Gyr for NGC 5822 and 0.8 Gyr for IC 4756. However, especially in the case of IC 4756, new photometry will considerably reduce the uncertainties. This is of crucial importance owing to the impact of the ages of these clusters on the characterization of the evolution of chromospheric activity.

We compared lithium abundances with published cluster data at 3 different ages, and with measurements made on stars in intermediate age clusters from our sample of Pace et al. (2008). Most of the stars studied by us have lithium abundance levels lying between that of NGC 752 and that of the Hyades-age clusters. We see evidence even though based on only 4 datapoints, that a steep decline in lithium abundances occurs below 6 000 K in IC 4651.

Clearly accurate determinations of temperature and lithium abundances in more member stars of such clusters as IC 4651 would be of value in understanding the reason for differences among clusters.

Acknowledgements. The quality of the paper improved due to the valuable comments of the referee, L. Pasquini. G. P. acknowledges L. Casagrande, M. Zoccali, L. Girardi and S. Recchi for useful discussions and S. Sousa for his kind support on ARES, his code for the automatic measurement of the equivalent widths. The data analysis performed here benefited from the impressive simplicity of use and efficiency of ARES. Data was collected at ESO, VLT. This publication made use of data products from the WEBDA database, created by J.-C. Mermilliod and now operated at the institute for Astronomy of the University of Vienna. The SIMBAD astronomical database and the NASA's Astrophysics Data System Abstract Service were also extensively used. G. P. acknowledges the support of the Fundação para a Ciência e a Tecnologia (Portugal) through the grant SFRH/BPD/39254/2007 and the project PTDC/CTE-AST/65971/2006.

References

- Alves-Brito, A., Meléndez, J., Asplund, M., Ramírez, I., & Yong, D. 2010, *A&A*, accepted
- Bensby, T., et al. 2009, arXiv:0911.5076, *A&A*, accepted
- Bragaglia, A., & Tosi, M. 2006, *AJ*, 131, 1544
- Carraro, G., Ng, Y. K., & Portinari, L. 1998, *MNRAS*, 296, 1045
- Carraro, G., Girardi, L., & Chiosi, C. 1999, *MNRAS*, 309, 430
- Carraro, G., Bresolin, F., Villanova, S., Matteucci, F., Patat, F., & Romaniello, M. 2004, *AJ*, 128, 1676
- Carraro, G., Geisler, D., Villanova, S., Frinchaboy, P. M., & Majewski, S. R. 2007, *A&A*, 476, 217
- Casagrande, L., Portinari, L., & Flynn, C. 2006, *MNRAS*, 373, 13
- De Silva, G. M., Gibson, B. K., Lattanzio, J., & Asplund, M. 2009, arXiv:0905.4354
- Dias, W. S., & Lépine, J. R. D. 2005, *ApJ*, 629, 825
- D'Orazi, V., & Randich, S. 2009, arXiv:0905.1835
- Edvardsson, B., Andersen, J., Gustafsson, B., Lambert, D. L., Nissen, P. E., & Tomkin, J. 1993, *A&A*, 275, 101
- Friel, E. D., Janes, K. A., Tavarez, M., Scott, J., Katsanis, R., Lotz, J., Hong, L., & Miller, N. 2002, *AJ*, 124, 2693
- Friel, E. D., Jacobson, H. R., Barrett, E., Fullton, L., Balachandran, S. C., & Pilachowski, C. A. 2003, *AJ*, 126, 2372
- Friel, E. D., Jacobson, H. R., & Pilachowski, C. A. 2005, *AJ*, 129, 2725
- Fulbright, J. P., McWilliam, A., & Rich, R. M. 2007, *ApJ*, 661, 1152
- Gilroy, K. K. 1989, *ApJ*, 347, 835
- Hakkila, J., Myers, J. M., Stidham, B. J., & Hartmann, D. H. 1997, *AJ*, 114, 2043
- Hekker, S., & Meléndez, J. 2007, *A&A*, 475, 1003
- Israelian, G., Santos, N. C., Mayor, M., & Rebolo, R. 2001, *Nature*, 411, 163
- Jacobson, H. R., Friel, E. D., & Pilachowski, C. A. 2007, *AJ*, 134, 1216
- Jacobson, H. R., Friel, E. D., & Pilachowski, C. A. 2009, *AJ*, 137, 4753
- Herzog, A. D., Sanders, W. L., & Seggewiss, W. 1975, *A&AS*, 19, 211
- Lecureur, A., Hill, V., Zoccali, M., Barbay, B., Gómez, A., Minniti, D., Ortolani, S., & Renzini, A. 2007, *A&A*, 465, 799
- Luck, R. E. 1994, *ApJS*, 91, 309
- Kurucz, R.L. 1993, *ATLAS9 Stellar Atmosphere Programs* (Kurucz CD-ROM No. 13)
- Magrini, L., Sestito, P., Randich, S., & Galli, D. 2009, *A&A*, 494, 95
- Mashonkina, L. I., Shimanskiĭ, V. V., & Sakhিবullin, N. A. 2000, *Astronomy Reports*, 44, 790
- Meléndez, J., Shchukina, N. G., Vasiljeva, I. E., & Ramírez, I. 2006, *ApJ*, 642, 1082
- Meléndez, J., et al. 2008, *A&A*, 484, L21
- Mermilliod, J.-C., & Mayor, M. 1990, *A&A*, 237, 61
- Mermilliod, J. C., Mayor, M., & Udry, S. 2008, *A&A*, 485, 303
- Pace, G., & Pasquini, L. 2004, *A&A*, 426, 1021
- Pace, G., Pasquini, L., & François, P. 2008, *A&A*, 489, 403
- Pace, G., Meléndez, J., Pasquini, L., Carraro, G., Danziger, J., François, P., Matteucci, F., & Santos, N. C. 2009, *A&A*, 499, L9
- Pasquini, L., Randich, S., Zoccali, M., Hill, V., Charbonnel, C., & Nordström, B. 2004, *A&A*, 424, 951
- Pasquini, L., Biazzo, K., Bonifacio, P., Randich, S., & Bedin, L. R. 2008, *A&A*, 489, 677
- Paulson, D. B., Sneden, C., & Cochran, W. D. 2003, *AJ*, 125, 3185
- Randich, S., Sestito, P., Primas, F., Pallavicini, R., & Pasquini, L. 2006, *A&A*, 450, 557
- Ryde, N., et al. 2010, *A&A*, 509, A260000
- Salaris, M., Weiss, A., & Percival, S. M. 2004, *A&A*, 414, 163
- Santos, N. C., Lovis, C., Pace, G., Meléndez, J., & Naef, D. 2009, *A&A*, 493, 309
- Schmidt, E. G. 1978, *PASP*, 90, 157
- Sestito, P., Randich, S., & Bragaglia, A. 2007, *A&A*, 465, 185
- Smiljanic, R., Pasquini, L., Charbonnel, C., & Lagarde, N. 2009, arXiv:0910.4399
- Snedden, C. 1973, *ApJ*, 184, 839
- Soderblom, D. R., Stauffer, J. R., Hudon, J. D., & Jones, B. F. 1993, *ApJS*, 85, 315
- Sousa, S. G., Santos, N. C., Israelian, G., Mayor, M., & Monteiro, M. J. P. F. G. 2007, *A&A*, 469, 783
- Sousa, S. G., et al. 2008, *A&A*, 487, 373
- Tautvaišienė, G., Edvardsson, B., Tuominen, I., & Ilyin, I. 2000, *A&A*, 360, 499
- Tautvaišienė, G., Edvardsson, B., Puzeras, E., & Ilyin, I. 2005, *A&A*, 431, 933
- Twarog, B. A., Anthony-Twarog, B. J., & McClure, R. D. 1993, *PASP*, 105, 78
- Villanova, S., Carraro, G., & Saviane, I. 2009, arXiv:0906.4330
- Xiong, D. R., & Deng, L. 2009, *MNRAS*, 395, 2013
- Zoccali, M., et al. 2006, *A&A*, 457, L1